



one without and one involving derivatives:

$$\begin{aligned} \mathcal{L}_{\text{int}} = & aK_0^{*-}\pi^0K^+ + bK_0^{*-}\partial_\mu\pi^0\partial^\mu K^+ \\ & + \sqrt{2}aK_0^{*-}\pi^+K^0 + \sqrt{2}bK_0^{*-}\partial_\mu\pi^+\partial^\mu K^0 + \dots, \end{aligned} \quad (1)$$

where dots represent analogous interaction terms for the other members of the isospin multiplets, as well as Hermitian conjugation. The decay width as function of the (running) mass  $m$  of the unstable  $K_0^*$  reads

$$\Gamma_{K_0^*}(m) = 3 \frac{k(m)}{8\pi m^2} \left[ a - b \frac{m^2 - m_\pi^2 - m_K^2}{2} \right]^2 F_\Lambda(m), \quad (2)$$

where the factor of 3 comes from summing over isospin. Here, we introduced the modulus of the three-momentum of the outgoing particles in the rest frame of the decaying particle as

$$\begin{aligned} k(m) = & \frac{\sqrt{m^4 + (m_\pi^2 - m_K^2)^2 - 2(m_\pi^2 + m_K^2)m^2}}{2m} \\ & \times \theta(m - m_\pi - m_K). \end{aligned} \quad (3)$$

The quantities  $m_\pi$  and  $m_K$  are the pion and kaon mass, respectively. The form factor  $F_\Lambda(m)$  is chosen as

$$F_\Lambda(m) = e^{-2k^2(m)/\Lambda^2}, \quad (4)$$

where  $\Lambda$  is an energy scale arising from the fact that mesons are not elementary objects (technically, it can be included already in the Lagrangian by making it non-local, see *e.g.* Ref. [33]). This parameter acts as a cutoff and assures that all our calculations are finite.

When the form factor is set to zero in Eq. (2) and  $m \simeq 1.43$  GeV, we obtain the so-called tree-level decay width. It can be identified with the physical width of the  $K_0^*(1430)$  in (some) phenomenological models, in which this resonance is interpreted as a quarkonium [32]. As we shall see, the bare seed state  $K_0^*$  in our Lagrangian (1) in fact corresponds roughly to the well-known resonance  $K_0^*(1430)$  – this is in agreement with various phenomenological studies of the scalar sector [7, 32, 34, 35].

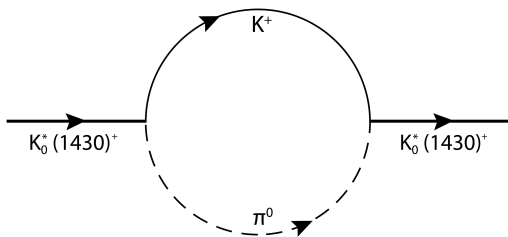


FIG. 1. Example of a one-loop contribution to  $\Pi(m)$ .

Following closely Ref. [36] (see also Refs. [16–18, 37]), we now briefly present the mathematical formalism. The propagator of the scalar kaonic field is given by

$$\Delta_{K_0^*}(p^2 = m^2) = \frac{1}{m^2 - m_0^2 - \Pi(m) + i\varepsilon}, \quad (5)$$

where  $m_0$  is the bare mass of the scalar kaon and  $\Pi(m)$  is the sum of all one-loop contributions with one pion and one kaon circulating in it, see Fig. 1. Although the loops in our model are regularized by the form factor in Eq. (4), one has to take into account emerging tadpole diagrams when using ordinary Feynman rules. The details are discussed in Ref. [36]. A study of the validity of the one-loop approximation was done in Ref. [38]. We will use that the spectral function is obtained from the propagator by

$$d_{K_0^*}(m) = -\frac{2m}{\pi} \text{Im} \Delta_{K_0^*}(p^2 = m^2), \quad (6)$$

having the correct normalization  $\int_0^\infty d_{K_0^*}(m) dm = 1$ , and that according to the optical theorem  $\text{Im} \Pi(m) = -m \Gamma_{K_0^*}(m)$ .

The  $J = 0$  and  $I = 1/2$  phase shift for  $\pi K$  scattering up to 1.8 GeV is assumed to be dominated by the scalar kaonic resonances(s). Within our framework it therefore takes the form (see the review of kinematics provided by the PDG [1])

$$\delta_{\pi K}(m) = \frac{1}{2} \arccos [1 - \pi \Gamma_{K_0^*}(m) d_{K_0^*}(m)]. \quad (7)$$

Some comments are in order:

(i) Eq. (7) is based on the assumption that the  $s$ -channel propagation dominates, *c.f.r.* Ref. [1]. The validity of this assumption (and thus neglecting the contributions from the  $u$ -channel exchange diagrams) was extensively discussed in the literature [39–41]. In particular, it was shown that this approximation alters only slightly the position of the resonance poles: it is therefore very suitable for our purposes.

(ii) Furthermore, the approximation of keeping only the  $s$ -channel is justified by the fact that we perform a fit to data starting at about 200 MeV above the  $\pi K$ -threshold. This is far enough from the threshold, where the overall interaction strength is small and all contributions are relevant (and where chiral symmetry is especially important, see also the considerations in the next point).

(iii) Note also that we do not use any constant background term in our model. This is different from many previous works on the subject (see *e.g.* Ref. [21] or, more recently, Ref. [26]); instead, we utilize derivative interactions. In order to illustrate this point, we introduce an analogy with the old linear sigma model, which contains a non-derivative interaction as well as a background term. The potential of the model has the usual Mexican hat form,  $V = \frac{\lambda}{4}(\pi^2 + \sigma^2 - F^2)^2 - \varepsilon\sigma$ . The field  $\sigma$  has a non-vanishing vacuum expectation value  $\phi$ ; as a consequence (after performing the shift  $\sigma \rightarrow \sigma + \phi$ ) the mass of  $\sigma$  reads  $M_\sigma^2 = \lambda\phi^2$ , while the pion mass reads  $M_\pi^2 = \varepsilon/\phi$  and vanishes in the chiral limit (where  $\varepsilon \propto m_q$  vanishes).

Retaining only the interaction terms relevant for  $\pi\pi$  scattering, we have  $V = \frac{\lambda}{4}\pi^4 + \lambda\sigma\pi^2 + \dots$ , thus one is left with a non-derivative interaction through  $\sigma$ -exchange, as well as a four-leg repulsion term. After transforming the

fields into a polar form by  $(\sigma, \vec{\pi}) \rightarrow \sigma e^{i\vec{t}\cdot\vec{\pi}}$  (an intermediate step toward chiral perturbation theory), we obtain  $V = \frac{1}{\phi}\sigma(\partial_\mu\vec{\pi})^2 - \frac{M_\pi^2}{2\phi}\sigma\vec{\pi}^2 + \dots$ , *i.e.*, no background term of type  $\vec{\pi}^4$  is present, but a dominant derivative interaction has emerged.

The non-derivative interaction is subdominant and vanishes in the chiral limit: this is in agreement with low-energy chiral theorems. The interchange of one pion field with one kaon field allows us to pass from the case of the  $\sigma$  to that of the kaonic sector studied here (formally, it is a simple rotation in flavor space), but the very same intuitive arguments show why the use of derivative interactions is important for scalar mesons in general. Moreover, the contemporary presence of derivative and non-derivative interactions implies that the structure giving rise to Adler's zero is automatically fulfilled (we thus do not have to add the Adler's zero separately, as done for example in Ref. [42]).

(*iv*) Our model is designed to study the scattering in the  $I = 1/2$  channel only, in which the  $s$ -wave exchange of a scalar kaon can be considered as dominant. Indeed, the scalar kaon contributes also through  $u$ -channel exchange diagrams to the cross-section. Experimentally, the  $I = 3/2$  phase shift is negative (*i.e.*, there is a repulsion in this channel) but is at least a factor of 4 smaller than for  $I = 1/2$ , showing also that the enhanced intensity in the  $I = 1/2$  channel can be ascribed to the  $s$ -wave exchange of a scalar kaon.

### III. RESULTS AND DISCUSSION

#### A. Our fit

The expression from Eq. (7) is fitted to the data of Ref. [20] with respect to the four model parameters  $a, b, \Lambda, m_0$ . The result is shown in Fig. 2 and the values of the parameters together with their errors are reported in Table I. The value of the  $\chi^2$  is fine:  $\chi_0^2/d.o.f. = 1.25$ , explaining the very good agreement of our model result with data. By comparing the coupling constants it turns out that the derivative coupling is dominant, which is expected by chPT [30] and by other studies [43].

By using the parameters listed in Table I we continue the propagator from Eq. (5) into the second Riemann sheet and scan the complex plane for poles. We find *two* poles (given in GeV) which we assign in the following way:

$$K_0^*(1430) : (1.413 \pm 0.002) - i(0.127 \pm 0.003), \quad (8)$$

$$K_0^*(800) : (0.746 \pm 0.019) - i(0.262 \pm 0.014). \quad (9)$$

Thus, a pole corresponding to the light  $\kappa$  emerges very naturally in our calculation and is a dynamically generated state (for a discussion on the definition of dynamical generation, see Refs. [44–46]). At this point, one should stress that the small errors quoted above (especially for what concerns the resonance  $K_0^*(1430)$ ) are specific to

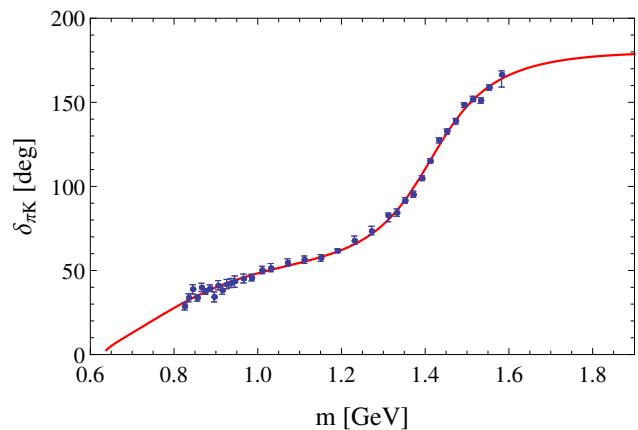


FIG. 2. The solid (red) curve shows our fit result for the phase shift from Eq. (7) with respect to the four model parameters  $a, b, \Lambda, m_0$  (see Table I). The blue points are the data of Ref. [20]. A very good agreement is obtained.

TABLE I. Results of the fit.  $\chi_0^2/d.o.f. = 1.25$

Parameter	Value
$a$	$1.60 \pm 0.22$ GeV
$b$	$-11.16 \pm 0.82$ GeV $^{-1}$
$\Lambda$	$0.496 \pm 0.008$ GeV
$m_0$	$1.204 \pm 0.008$ GeV

our model defined in Eqs. (1), (2), and (4), respectively. In particular, the choice of the form factor (4) is model dependent, a fact that introduces an intrinsic uncertainty. We will explore this point in more detail in the next subsection, in which the positions of the poles are studied for different modifications of the model.

The PDG [1] reports for  $K_0^*(1430)$  a mass of  $(1.425 \pm 0.050)$  GeV and a width of  $(0.270 \pm 0.080)$  GeV. Our values fit very well in these windows. In particular, our width, obtained by doubling the negative imaginary part of our pole, reads  $(0.254 \pm 0.006)$  GeV and is thus determined with a small error. For  $K_0^*(800)$  the PDG reports a mass of  $(0.682 \pm 0.029)$  GeV and a width of  $(0.547 \pm 0.024)$  GeV, which are also in agreement with our values (although our results point to a somewhat larger value for the mass). The mass  $(0.746 \pm 0.019)$  GeV and width  $(0.524 \pm 0.028)$  GeV determined within our model are also in good agreement with most of the pole determinations listed in Ref. [1].

In the left panel of Fig. 3 we show the spectral function for the parameters of Table I. A low-energy enhancement is present, but no peak. The absence of a peak is one of the reasons why the acceptance of the  $\kappa$  might be considered to be controversial. However, if resonance poles on unphysical Riemann sheets are the relevant quantities, it turns out that the existence of the broad  $\kappa$  is a consequence of our model.

Similar statements can be made concerning the broad

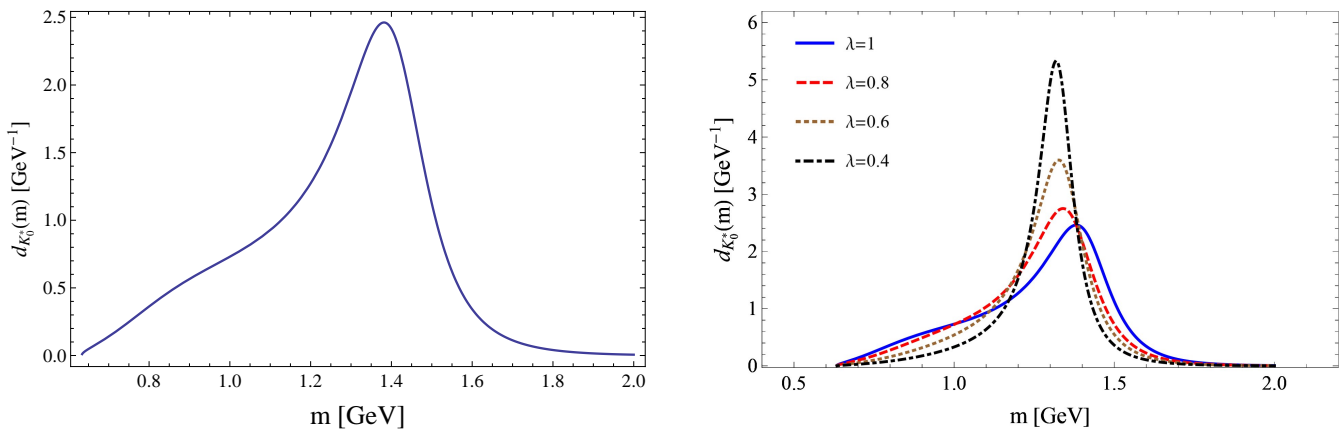


FIG. 3. In the left panel we show the spectral function from Eq. (6) plotted for the parameters of Table I. An enhancement for low values of the running mass  $m$  is clearly visible. In the right panel we show the spectral function for different values of the scaling parameter  $\lambda = 3/N_c$ . The smaller  $\lambda$  is, the more peaked is the spectral function and the enhancement for low values of the running mass decreases.

isoscalar state  $f_0(500)$ : its pole is widely accepted while a clear peak in the spectral function is not present. On the contrary, the two scalar states  $a_0(980)$  and  $f_0(980)$  are pretty narrow: although their couplings are large, these resonances sit just at the kaon-kaon threshold, making their decays into kaons to be kinematically suppressed. In conclusion, all those states together with  $\kappa$  seem to have their common origin in quantum fluctuations.

We also study the change of the spectral function and of the position of the poles when performing a rescaling of the coupling constants:

$$a \rightarrow \sqrt{\lambda}a, \quad b \rightarrow \sqrt{\lambda}b \quad \text{with } \lambda \leq 1. \quad (10)$$

This is completely equivalent to a large- $N_c$  study upon setting

$$\lambda = \frac{3}{N_c}. \quad (11)$$

The spectral function is plotted in the right panel of Fig. 3 for different values of  $\lambda$ . Obviously, the low-energy enhancement becomes smaller for decreasing  $\lambda$ , *i.e.*, for increasing  $N_c$ .

Finally, we present the pole movement as function of  $\lambda$  in Fig. 4. We observe that the pole of  $K_0^*(1430)$  moves toward the real axis, a behavior expected for a quarkonium state. The pole of  $K_0^*(800)$  moves away from the real axis and disappears for  $\lambda \simeq 0.24$  (or  $N_c \simeq 13$ ). From this it follows that the pole of  $K_0^*(800)$  is dynamically generated and does not survive in the large- $N_c$  limit. Such a behavior was also reported in Refs. [10, 42, 47, 48].

It should be stressed at this point that the choice of the form factor (4) is model dependent. A Gaussian form as implemented here is a standard choice when investigating mesonic resonances and the position of their poles, respectively, see also the discussion in Refs. [39–41]. Yet, in Sec. III B we investigate possible variations of the form

factor and indeed find that they are not capable of reproducing the phase shift data correctly. At the same time, we will also investigate the statistical significance of the fit presented in this subsection as well as the fits that we will discuss in Sec. III B.

## B. Variations of the model

In this subsection we investigate different scenarios in order to understand better how the results discussed in the previous part emerge. We first perform two fits to the phase shift data: one in which we consider only the non-derivative term in Eq. (1) (we set  $b = 0$ ), and one in which we consider only the derivative term (we set  $a = 0$ ).

The results are presented in the left panel of Fig. 5 and

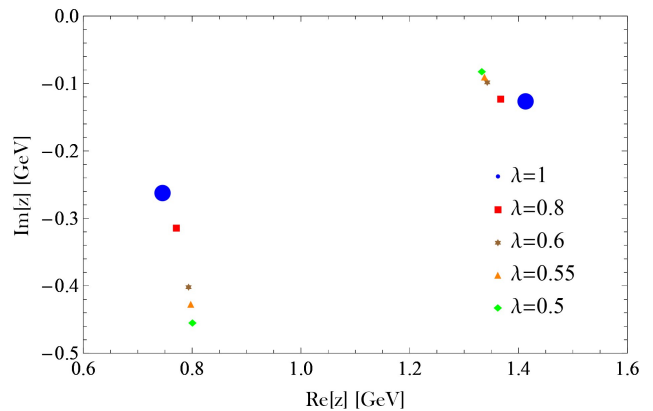


FIG. 4. Movement of the two resonance poles for different values of  $\lambda = 3/N_c$ . While the pole corresponding to  $K_0^*(1430)$  moves toward the real axis, the pole of the light  $K_0^*(800)$  moves away from the real axis and disappears for  $\lambda \simeq 0.24$ .

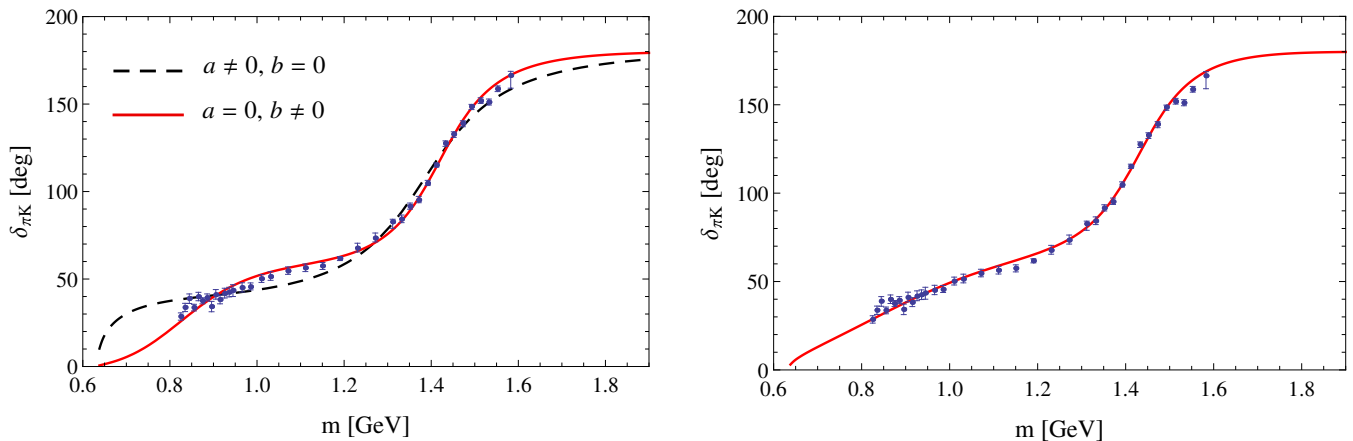


FIG. 5. Left panel: The solid (red) and dashed (black) curves show our fit results for the phase shift from Eq. (7) with respect to the four model parameters  $a, b, \Lambda, m_0$  (see Table II). The blue points are the usual data of Ref. [20]. Right panel: The solid (red) curve shows the fit for the modified form factor in Eq. (13).

in Table II. The first entry summarizes what was found in the previous subsection. The second and third entries represent the two cases  $b = 0$  and  $a = 0$ , respectively. As can be seen in the third column, in both cases the  $\chi^2$  has increased, signaling a worse agreement than with our first fit.

Yet, in order to be more quantitative, we report in the fourth column the results of a statistical test of the goodness of the fit: The quantity

$$p(\chi^2 > \chi_0^2) = \frac{1}{2^{d/2}\Gamma(d/2)} \int_{\chi_0^2}^{\infty} dx x^{d/2-1} e^{-x/2} \quad (12)$$

(with  $d = d.o.f.$ ) is the probability to obtain a larger value of the  $\chi^2$  than  $\chi_0^2$  if a new experiment shall be performed (by using, of course, the same theoretical function in the fit). When this probability is very small, one may conclude that (i) the theoretical model is not correct (a reasonable conclusion) or (ii) the theoretical model is correct but the experimental results show a – quite unlucky – statistical fluctuation. When this probability is, for instance, smaller than 5%, one can exclude the theoretical model at the 95% confidence level. In our case, our preferred solution from the previous subsection gives  $p(\chi^2 > \chi_0^2) = 15.3\%$ , which implies that the theoretical model *cannot* be rejected (here,  $d.o.f. = 37 - 4 = 33$ ). On the contrary, the models with only non-derivative interactions and with derivative interactions can be rejected with a very high level of accuracy. While this result is expected for the non-derivative term because the shape of the theoretical function does not match the data (see left panel of Fig. 5), the situation is more subtle in the case of only derivative terms. Here, the form is by-eye qualitatively correct, but the statistical test shows that it is not in agreement with the experiment (with  $d.o.f. = 37 - 3 = 34$ ).

Finally, in the fifth and sixth columns we report for completeness the position of the poles for the various

models. Yet, in view of the statistical analysis, only the first row can be regarded as reliable.

As a next step we investigate other types of the form factor. As explained before, the Gaussian form factor is rather standard in various works on the subject and it is also easy to use. Especially in presence of derivative interactions it is very practical since it cuts off the integrand in the loop integral sufficiently fast [49]. However, there is no fundamental reason why the Gaussian should be the best one to apply. It is therefore important to check variations of it. We test the following simple modification:

$$F_{\Lambda}(m) = e^{-2k^4(m)/\Lambda^4}. \quad (13)$$

The result of the fit is reported in the right panel of Fig. 5 as well as in the last entry of Table II. Also in this case, the right panel of Fig. 5 shows a qualitative agreement of the model with data. Yet, the statistical test excludes this model at a very high-level of accuracy. From this perspective it is not surprising to find the pole of the  $\kappa$  to be not in agreement with our result in the previous subsection and with other listings in the PDG. Thus, changing the form factor does not guarantee a good description of data, especially for what concerns the  $\kappa$ .

We have also tried a Fermi function  $F_{\Lambda}(m) = [(1 + e^{-\alpha\Lambda^2})/(1 + e^{\alpha(k^2(m)-\Lambda^2)})]^2$  for various values of the parameter  $\alpha$ . This form factor is approximately constant for small  $k$  and rapidly decreases to zero for  $k \sim \Lambda$  (the higher  $\alpha$ , the steeper the descent; for  $\alpha \rightarrow \infty$  the Heaviside step-function is realized). But also for this choice it was not possible to obtain a fit which would pass the statistical test of the  $\chi^2$ .

In conclusion, our study confirms that the Gaussian form factor is an adequate choice for mesonic interactions, leading to results that are in a good agreement with the data up to  $\sim 1.8$  GeV, when *both* a (dominant) derivative and a (subdominant) non-derivative interaction term are *simultaneously* taken into account.

TABLE II. Fitting results for the variations of the model.

Scenario	Parameters	$\chi_0^2/d.o.f.$	$p(\chi^2 > \chi_0^2)$	Pole for $K_0^*(800)$	Pole for $K_0^*(1430)$
$a, b \neq 0$ , Gaussian	$a = 1.60 \pm 0.22$ GeV	1.25	0.15	$(0.746 \pm 0.019)$ $-i(0.262 \pm 0.014)$	$(1.413 \pm 0.002)$ $-i(0.127 \pm 0.003)$
	$b = -11.16 \pm 0.82$ GeV $^{-1}$				
	$\Lambda = 0.496 \pm 0.008$ GeV				
	$m_0 = 1.204 \pm 0.008$ GeV				
$b = 0$ , Gaussian	$a = 4.06 \pm 0.04$ GeV	5.41	$1.72 \cdot 10^{-22}$	-	$(1.385 \pm 0.002)$ $-i(0.146 \pm 0.003)$
	$\Lambda = 0.902 \pm 0.015$ GeV				
	$m_0 = 1.299 \pm 0.002$ GeV				
$a = 0$ , Gaussian	$b = -17.10 \pm 0.17$ GeV $^{-1}$	2.54	$1.92 \cdot 10^{-6}$	$(0.820 \pm 0.003)$ $-i(0.187 \pm 0.002)$	$(1.419 \pm 0.001)$ $-i(0.112 \pm 0.002)$
	$\Lambda = 0.453 \pm 0.002$ GeV				
	$m_0 = 1.142 \pm 0.002$ GeV				
$a, b \neq 0$ , $F_\Lambda(m) = e^{-2k^4(m)/\Lambda^4}$	$a = 2.32 \pm 0.09$ GeV	2.86	$7.98 \cdot 10^{-8}$	$(0.863 \pm 0.008)$ $-i(0.339 \pm 0.017)$	$(1.433 \pm 0.002)$ $-i(0.112 \pm 0.003)$
	$b = -3.40 \pm 0.26$ GeV $^{-1}$				
	$\Lambda = 0.652 \pm 0.006$ GeV				
	$m_0 = 1.248 \pm 0.003$ GeV				

#### IV. CONCLUSIONS

The scalar sector of hadron physics has been in the center of debate both from the theoretical and experimental side since a long time. There seems to be a consensus nowadays that at least the scalar states below 1 GeV are non-conventional mesons [19, 44]. In particular, the role of hadronic loop contributions to the self-energy, such as the one in Fig. 1, has been found to be crucial in various studies [8–18, 37].

We have concentrated in this work on the channel  $I = 1/2$ ,  $J = 0$ . Our model contains non-derivative and derivative interactions in agreement with effective approaches of low-energy QCD [30, 32]. It was demonstrated that, by using a single kaonic seed state, both scalar resonances  $K_0^*(1430)$  and  $K_0^*(800)$  (known as  $\kappa$ ) can be described as complex propagator poles. The two poles are required in order to correctly reproduce phase shift data of  $\pi K$  scattering. The spectral function of our model turns out to be not of the ordinary Breit–Wigner type, too, due to strong distortions in the low-energy regime, which are a direct consequence of the  $\kappa$ -pole.

In the large- $N_c$  limit this pole finally disappears;

the corresponding state is therefore not a conventional quarkonium. On the contrary, the pole corresponding to  $K_0^*(1430)$  approaches the real energy axis for large values of  $N_c$ , hence becomes very narrow, which is a general feature of a quark-antiquark state.

It must be stressed that the presence of derivative interactions is crucial for our results. They turn out to be the dominant contribution toward the description of the  $\pi K$  phase shift. For the future, one should use more complete models than the one presented in this work. In particular, a model is desired which allows to study simultaneously the  $I = 1/2$  and the  $I = 3/2$  channels. For instance, the extended Linear Sigma Model of Ref. [32], that was used here as a motivation for our Lagrangian with derivative and non-derivative terms, can be applied for this purpose. Preliminary results in this direction are encouraging: In the  $I = 1/2$  sector this more complete hadronic model reduces – also for what concerns the numerical values – to the Lagrangian of Eq. (1).

#### ACKNOWLEDGMENTS

T.W. acknowledges financial support from HGS-HIRE, F&E GSI/GU, and HIC for FAIR Frankfurt.

- [1] K. A. Olive *et al.* (Particle Data Group), *Chin. Phys. C* **38**, 090001 (2014).
- [2] J. R. Peláez, (2015), arXiv:1510.00653 [hep-ph].
- [3] R. L. Jaffe, *Phys. Rev. D* **15**, 267 (1977); **15**, 281 (1977).
- [4] R. L. Jaffe, *Phys. Rep.* **409**, 1 (2005), arXiv:hep-ph/0409065.
- [5] L. Maiani, F. Piccinini, A. D. Polosa, and V. Ri-

quer, *Phys. Rev. Lett.* **93**, 212002 (2004), arXiv:hep-ph/0407017.

- [6] F. Giacosa, *Phys. Rev. D* **74**, 014028 (2006), arXiv:hep-ph/0605191; **75**, 054007 (2007), arXiv:hep-ph/0611388; F. Giacosa and G. Pagliara, *Nucl. Phys. A* **833**, 138 (2010), arXiv:0905.3706 [hep-ph].
- [7] A. H. Fariborz, R. Jora, and J. Schechter, *Phys. Rev.*

- D **72**, 034001 (2005), arXiv:hep-ph/0506170; A. H. Fariborz, Int. J. Mod. Phys. A **19**, 2095 (2004), arXiv:hep-ph/0302133; M. Napsuciale and S. Rodriguez, Phys. Rev. D **70**, 094043 (2004), arXiv:hep-ph/0407037; A. H. Fariborz, A. Azizi, and A. Asrar, (2015), arXiv:1511.02449 [hep-ph].
- [8] F. E. Close and N. A. Törnqvist, J. Phys. G **28**, R249 (2002), arXiv:hep-ph/0204205.
- [9] J. R. Peláez and G. Ríos, Phys. Rev. Lett. **97**, 242002 (2006), arXiv:hep-ph/0610397; J. R. Peláez, **92**, 102001 (2004), arXiv:hep-ph/0309292.
- [10] J. R. Peláez, Mod. Phys. Lett. A **19**, 2879 (2004), arXiv:hep-ph/0411107.
- [11] J. A. Oller and E. Oset, Nucl. Phys. A **620**, 438 (1997), [Erratum-ibid. 652, 407 (1999)], arXiv:hep-ph/9702314; J. A. Oller, E. Oset, and J. R. Peláez, Phys. Rev. Lett. **80**, 3452 (1998), arXiv:hep-ph/9803242; Phys. Rev. D **59**, 074001 (1999), [Erratum-ibid. 60, 099906 (1999); Erratum-ibid. 75, 099903 (2007)], arXiv:hep-ph/9804209.
- [12] J. A. Oller and E. Oset, Phys. Rev. D **60**, 074023 (1999), arXiv:hep-ph/9809337.
- [13] M. Jamin, J. A. Oller, and A. Pich, Nucl. Phys. B **587**, 331 (2000), arXiv:hep-ph/0006045; M. Albaladejo and J. A. Oller, Phys. Rev. Lett. **101**, 252002 (2008), arXiv:0801.4929 [hep-ph].
- [14] E. van Beveren, D. V. Bugg, F. Kleefeld, and G. Rupp, Phys. Lett. B **641**, 265 (2006), arXiv:hep-ph/0606022.
- [15] D. Morgan and M. R. Pennington, Phys. Rev. D **48**, 1185 (1993).
- [16] E. van Beveren, T. A. Rijken, K. Metzger, C. Dullemond, G. Rupp, and J. E. Ribeiro, Z. Phys. C **30**, 615 (1986), arXiv:0710.4067 [hep-ph].
- [17] N. A. Törnqvist, Z. Phys. C **68**, 647 (1995), arXiv:hep-ph/9504372; N. A. Törnqvist and M. Roos, Phys. Rev. Lett. **76**, 1575 (1996), arXiv:hep-ph/9511210v1.
- [18] M. Boglione and M. R. Pennington, Phys. Rev. Lett. **79**, 1998 (1997), arXiv:hep-ph/9703257; Phys. Rev. D **65**, 114010 (2002), arXiv:hep-ph/0203149.
- [19] C. Amsler and N. A. Törnqvist, Phys. Rep. **389**, 61 (2004); E. Klempt and A. Zaitsev, **454**, 1 (2007), arXiv:0708.4016 [hep-ph].
- [20] D. Aston *et al.*, Nucl. Phys. B **296**, 493 (1988).
- [21] S. Ishida, M. Ishida, T. Ishida, K. Takamatsu, and T. Tsuru, Prog. Theor. Phys. **98**, 621 (1997), arXiv:hep-ph/9705437.
- [22] P. C. Magalhães *et al.*, Phys. Rev. D **84**, 094001 (2011), arXiv:1105.5120 [hep-ph].
- [23] S. Descotes-Genon and B. Moussalam, Eur. Phys. J. C **48**, 553 (2006), arXiv:hep-ph/0607133.
- [24] H. Q. Zheng, Z. Y. Zhou, G. Y. Qin, Z. G. Xiao, J. J. Wang, and N. Wu, Nucl. Phys. A **733**, 235 (2004), arXiv:hep-ph/0310293; Z. Y. Zhou and H. Q. Zheng, **775**, 212 (2006), arXiv:hep-ph/0603062.
- [25] D. Black, A. H. Fariborz, F. Sannino, and J. Schechter, Phys. Rev. D **58**, 054012 (1998), arXiv:hep-ph/9804273.
- [26] A. H. Fariborz, E. Pourjafarabadi, S. Zarepour, and S. M. Zebarjad, Phys. Rev. D **92**, 113002 (2015), arXiv:1511.01623 [hep-ph].
- [27] T. Ledwig, J. Nieves, A. Pich, E. R. Arriola, and J. R. de Elvira, Phys. Rev. D **90**, 114020 (2014), arXiv:1407.3750 [hep-ph].
- [28] M. Ablikim *et al.* (BES Collaboration), Phys. Lett. B **698**, 183 (2011), arXiv:1008.4489 [hep-ex].
- [29] Z. Fu, JHEP **01**, 017 (2012), arXiv:1110.5975 [hep-lat].
- [30] J. Gasser and H. Leutwyler, Ann. Phys. **158**, 142 (1984); G. Ecker, J. Gasser, A. Pich, and E. D. Rafael, Nucl. Phys. B **321**, 311 (1989); S. Scherer, Adv. Nucl. Phys. **27**, 277 (2003), arXiv:hep-ph/0210398.
- [31] P. Ko and S. Rudaz, Phys. Rev. D **50**, 6877 (1994); M. Urban, M. Buballa, and J. Wambach, Nucl. Phys. A **697**, 338 (2002), arXiv:hep-ph/0102260.
- [32] D. Parganlija, P. Kovacs, G. Wolf, F. Giacosa, and D. H. Rischke, Phys. Rev. D **87**, 014011 (2013), arXiv:1208.0585 [hep-ph].
- [33] J. Terning, Phys. Rev. D **44**, 887 (1991); A. Faessler, T. Gutsche, M. A. Ivanov, V. E. Lyubovitskij, and P. Wang, **68**, 014011 (2003), arXiv:hep-ph/0304031.
- [34] C. Amsler and F. E. Close, Phys. Rev. D **53**, 295 (1996), arXiv:hep-ph/9507326; F. E. Close and A. Kirk, Eur. Phys. J. B **21**, 531 (2001), arXiv:hep-ph/0103173; F. Giacosa, T. Gutsche, V. E. Lyubovitskij, and A. Faessler, Phys. Lett. B **622**, 277 (2005), arXiv:hep-ph/0504033; Phys. Rev. D **72**, 094006 (2005), arXiv:hep-ph/0509247.
- [35] S. Godfrey and N. Isgur, Phys. Rev. D **32**, 189 (1985).
- [36] T. Wolkanowski, F. Giacosa, and D. H. Rischke, Phys. Rev. D **93**, 014002 (2016), arXiv:1508.00372 [hep-ph].
- [37] F. Giacosa and G. Pagliara, Phys. Rev. C **76**, 065204 (2007), arXiv:0707.3594 [hep-ph]; F. Giacosa and T. Wolkanowski, Mod. Phys. Lett. A **27**, 1250229 (2012), arXiv:1209.2332 [hep-ph].
- [38] J. Schneider, T. Wolkanowski, and F. Giacosa, Nucl. Phys. B **888**, 287 (2014), arXiv:1407.7414 [hep-ph].
- [39] N. Isgur and J. Speth, Phys. Rev. Lett. **77**, 2332 (1996); N. A. Törnqvist and M. Roos, **77**, 2333 (1996).
- [40] M. Harada, F. Sannino, and J. Schechter, Phys. Rev. Lett. **78**, 1603 (1997), arXiv:hep-ph/9609428; N. A. Törnqvist and M. Roos, **78**, 1604 (1997), arXiv:hep-ph/9610527.
- [41] G. Rupp, E. van Beveren, and M. D. Scadron, Phys. Rev. D **65**, 078501 (2002), arXiv:hep-ph/0104087.
- [42] Z.-Y. Zhou and Z. Xiao, Phys. Rev. D **83**, 014010 (2011), arXiv:1007.2072 [hep-ph].
- [43] D. Black, M. Harada, and J. Schechter, Phys. Rev. D **73**, 054017 (2006), arXiv:hep-ph/0601052; F. Giacosa and G. Pagliara, Nucl. Phys. A **812**, 125 (2008), arXiv:0804.1572 [hep-ph].
- [44] F. Giacosa, Phys. Rev. D **80**, 074028 (2009), arXiv:0903.4481 [hep-ph].
- [45] Z.-H. Guo and J. A. Oller, (2015), arXiv:1508.06400 [hep-ph].
- [46] M. Albaladejo and J. A. Oller, Phys. Rev. D **86**, 034003 (2012), arXiv:1205.6606 [hep-ph].
- [47] Z.-H. Guo and J. A. Oller, Phys. Rev. D **84**, 034005 (2011), arXiv:1104.2849 [hep-ph].
- [48] Z.-H. Guo, J. A. Oller, and J. R. de Elvira, Phys. Rev. D **86**, 054006 (2012), arXiv:1206.4163 [hep-ph].
- [49] When using a form like  $(1 + k^n/\Lambda^n)^{-2}$  one usually observes non-physical bumps at high energies [6].